LMR: Lane Distance-Based Metric for Trajectory Prediction

Julian Schmidt[*†], Thomas Monninger[‡], Julian Jordan[*] and Klaus Dietmayer[†]

[*]Mercedes-Benz AG, Research & Development, Stuttgart, Germany

Email: julian.sj.schmidt@mercedes-benz.com

[†]Ulm University, Institute of Measurement, Control and Microtechnology, Ulm, Germany

[‡]Mercedes-Benz Research & Development North America, Sunnyvale, CA, USA

Abstract—The development of approaches for trajectory prediction requires metrics to validate and compare their performance. Currently established metrics are based on Euclidean distance, which means that errors are weighted equally in all directions. Euclidean metrics are insufficient for structured environments like roads, since they do not properly capture the agent's intent relative to the underlying lane. In order to provide a reasonable assessment of trajectory prediction approaches with regard to the downstream planning task, we propose a new metric that is lane distance-based: Lane Miss Rate (LMR). For the calculation of LMR, the ground-truth and predicted endpoints are assigned to lane segments, more precisely their centerlines. Measured by the distance along the lane segments, predictions that are within a certain threshold distance to the ground-truth count as hits, otherwise they count as misses. LMR is then defined as the ratio of sequences that yield a miss. Our results on three state-of-the-art trajectory prediction models show that LMR preserves the order of Euclidean distance-based metrics. In contrast to the Euclidean Miss Rate, qualitative results show that LMR yields misses for sequences where predictions are located on wrong lanes. Hits on the other hand result for sequences where predictions are located on the correct lane. This means that LMR implicitly weights Euclidean error relative to the lane and goes into the direction of capturing intents of traffic agents. The source code of LMR for Argoverse 2 is publicly available[1].

Index Terms—Behavior-Based Systems, Motion and Path Planning, AI-Based Methods

I. Introduction

In order to plan their future motion, autonomous vehicles are required to predict the motion of surrounding agents. Recently, there has been a large amount of interest in learning-based trajectory prediction, resulting in a myriad of different approaches, e.g., predicting trajectories based on a vectorized [1]–[3] or rasterized [4], [5] scene representation.

Given this variety of approaches, also methods that allow a quantitative comparison are required. For this purpose, prediction metrics, such as Average Displacement Error (ADE), Final Displacement Error (FDE) and Miss Rate (MR), exist.

These currently established prediction metrics are based on the Euclidean distance between ground-truth and predictions. We argue that measuring prediction performance solely by

(a) Euclidean distance-based Miss Rate
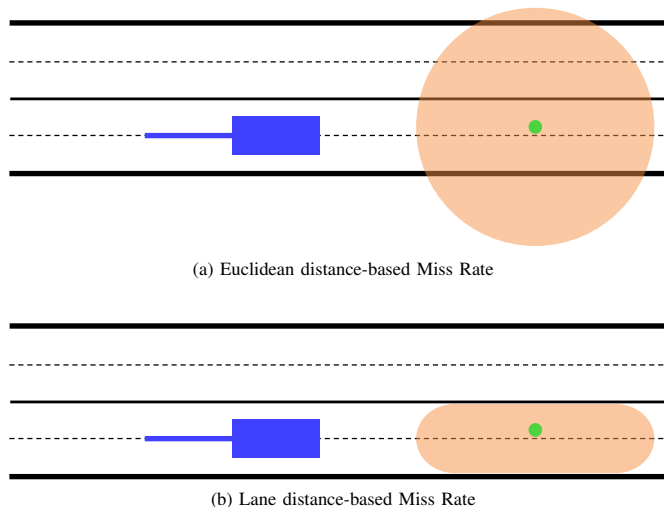

(b) Lane distance-based Miss Rate

Fig. 1. Overview of the established (a) Euclidean distance-based Miss Rate and our (b) lane distance-based Miss Rate: The green point indicates the ground-truth endpoint. Predictions within the orange area result in a hit and vice versa. Lane centerlines are illustrated with dashed lines.

means of spatial distance is insufficient since it does not account for different effects of a displacement at different directions, e.g., due to variations in lane geometry and traffic regulations. As an example, in some cases, a Euclidean error in longitudinal direction is considerably less severe than the same Euclidean error in lateral distance, which might yield a prediction that is located on the oncoming opposing lane. Under consideration of the downstream planning task, this means that the same Euclidean error can yield to significantly different results. Hence, Euclidean error has an asymmetrical effect on the downstream planning task.

In this paper, we propose a lane distance-based metric for the evaluation of trajectory prediction models. For the calculation of this metric, ground-truth and predicted endpoints are assigned to lane segments. Measured by the distance along the lane segments, predictions that are within a certain threshold distance to the ground-truth count as hits and predictions that are outside that threshold distance count as misses.

Fig. 1 illustrates how this compares to the already existing Euclidean distance-based MR. The (a) Euclidean distance-based MR yields hits even for predictions on opposing lanes and outside of the drivable space. Our (b) lane distance-based

MR, however, aims to consider asymmetrical effects by only yielding hits for predictions that are assigned to the same lane segment as the ground-truth. This way, our metric goes into the direction of capturing intents of traffic agents.

In summary, our main contributions are:

- We propose Lane Miss Rate (LMR), a novel lane distance-based metric for the evaluation of trajectory prediction models.
- We extensively compare different state-of-the-art trajectory prediction models on already established metrics and on our newly introduced LMR.
- We provide publicly available source code of LMR for Argoverse 2 and therefore contribute to the field of trajectory prediction evaluation.

II. RELATED WORK

This section describes related work regarding the evaluation of trajectory prediction models. Existing methods are grouped into accuracy-based metrics, quality metrics and planning-based metrics.

A. Accuracy-Based Metrics

Accuracy-based metrics are mainly Euclidean distance-based and are the most established metrics used for the evaluation of trajectory prediction models [6]–[8]. The minimum Average Displacement Error (minADE) and minimum Final Displacement Error (minFDE) are metrics introduced in early work related to learning-based trajectory prediction [6], [9]–[12]. minFDE is the Euclidean distance between the ground-truth endpoint and the predicted endpoint. For multi-modal predictions, only the prediction with the shortest distance is considered. minADE is the average Euclidean distance between the ground-truth and the predicted trajectory, with multi-modal predictions being evaluated with the same trajectory used for the calculation of the minFDE. For multi-modal predictions with probability estimates per mode, brier-minADE and brier-minFDE are applicable [13]. They correspond to the term $(1-p)^2$ being added to the minADE and minFDE value. The term considers the probability p of the mode selected for the minADE and minFDE calculation.

Miss Rate (MR) is the ratio of sequences, where the Euclidean prediction error is larger than a defined threshold [9], [14]. Most commonly, the prediction error refers to the Euclidean endpoint error and the threshold is a predefined distance, e.g., $2\,\mathrm{m}$ [6], [8]. For multi-modal predictions, all modes must be above the threshold, in order to yield a miss. Using separate Euclidean thresholds for longitudinal and lateral directions that are additionally dependent on time and velocity is also possible [7].

Other noteworthy Euclidean distance-based metrics are mean Average Precision (mAP) [7], which is based on MR, and Negative Log Likelihood (NLL) [15], which additionally considers positional uncertainty in predictions.

Our proposed metric is also accuracy-based. However, in contrast to already exiting accuracy-based metrics, it is dependent on the lane distance instead of pure Euclidean distance.

B. Quality Metrics

Alternatively, it is possible to measure the quality of a predicted trajectory without considering the ground-truth. Turn Rate Infeasibility (TRI) is used to measure the ratio of predictions that are kinematically infeasible in terms of the predicted turn radius [16]. Off-road rate and Drivable Area Compliance (DAC) measure the quality of predictions by determining whether a prediction lies within the drivable space given by a map or not [6].

Quality metrics by no means replace existing distance-based metrics. They only serve as an additional criterion to check for certain requirements (e.g., kinematically feasible predictions), which is why they are not well established.

C. Planning-Based Metrics

Instead of directly quantifying prediction performance, it is also possible to measure the performance of a planner that utilizes these predictions. Planning KL Divergence (PKL) is a metric that allows for such a comparison [17]. PKL is used to compare the output of a planner dependent on different object detectors to the output of the same planner using ground-truth objects. Instead of comparing the planner performance dependent on different object detectors, this principle would also allow for the comparison of the planner performance dependent on different prediction models. Downside is that prediction performance is not measured in an isolated way.

An alternative approach is to only work with a planner-agnostic cost function for planning [18]. Relying on continuous inverse optimal control to learn weights of the cost function from a large-scale dataset makes this approach dependent on the distribution of the dataset used for learning.

While these planning-based metrics aim to not suffer from the asymmetries of Euclidean distance-based metrics, we argue that simplicity is still an important criterion for the applicability of metrics. Using planners or planner cost functions is complex to implement and introduces additional dependencies on the planner or the cost function, which is why these metrics are not well established.

III. PROBLEM DEFINITION

We define the ground-truth future trajectory of an agent as $\mathbf{T}_{\mathrm{gt}} = \{\boldsymbol{\tau}^t\}_{t=1}^{T_f}$, with T_f being the prediction horizon. Predictions of a trajectory prediction model are denoted as $\mathbf{T}_{\mathrm{pred}} = \{\mathbf{T}_{\mathrm{pred},i}\}_{i=1}^{k}$, with $\mathbf{T}_{\mathrm{pred},i} = \{\tilde{\boldsymbol{\tau}}_i^t\}_{t=1}^{T_f}$. The index $i \in 1, \ldots, k$ considers the multi-modality of future motion by including k predicted modes.

The evaluation of trajectory prediction models comes down to finding a measure of quality for $\mathbf{T}_{\mathrm{pred}}$, possibly depending on $\mathbf{T}_{\mathrm{gt}}$.

IV. METHOD

This section describes LMR, our lane distance-based trajectory prediction evaluation metric.

Algorithm 1 Lane miss calculation for multi-modal predictions

1: **Input**
2:     $\mathbf{T}_{\text{gt}}$ Ground-truth future trajectory
3:     $\mathbf{T}_{\text{pred}}$ Predicted future trajectories
4:     $\mathcal{G}$ Lane graph
5: **Output**
6:     $\mathbf{x}$ Is miss
7: **procedure** GET_IS_MISS($\mathbf{T}_{\text{gt}}, \mathbf{T}_{\text{pred}}, \mathcal{G}$)
8:     Calculate average ground-truth velocity: v_{gt}
9:     Calculate velocity-dependent lane hit threshold: $s_{\text{hit}} \leftarrow (c_{\text{scale}} \cdot v_{\text{gt}}) + c_{\text{const}}$ ▷ We use $c_{\text{scale}} = 0.2\,\text{s}$ and $c_{\text{const}} = 0.7\,\text{m}$
10:    Calculate most probable lane assignment of $\mathbf{T}_{\text{gt}}$: $l_{\text{gt}}, s_{\text{gt}}, p_{\text{gt}} \leftarrow \max\limits_{p} (\text{GET\_LANE\_ASSIGNMENTS}(\mathbf{T}_{\text{gt}}, \mathcal{G}))$
11:    Initialize empty miss list: $\mathbf{x} \leftarrow [\,]$
12:    **for** $\mathbf{T}_{\text{pred},i}$ in $\mathbf{T}_{\text{pred}}$ **do**
13:        Calculate all N lane assignments of $\mathbf{T}_{\text{pred},i}$:
              $[(l_{\text{pred},i,1}, s_{\text{pred},i,1}, p_{\text{pred},i,1}), \dots, (l_{\text{pred},i,N}, s_{\text{pred},i,N}, p_{\text{pred},i,N})] \leftarrow \text{GET\_LANE\_ASSIGNMENTS}(\mathbf{T}_{\text{pred},i}, \mathcal{G})$
                                        ▷ We only use assignments where $p_{\text{pred},i,n}$ is at most 0.1 smaller than $\max(p_{\text{pred},i,n})$
14:        **if** (Distance along $\mathcal{G}$ from lane segment l_{gt} at value s_{gt} to any lane segment $l_{\text{pred},i,n}$ at value $s_{\text{pred},i,n}$) $< s_{\text{hit}}$ **then**
15:            $\mathbf{x}$.insert(0) **else** $\mathbf{x}$.insert(1) **end if**
16:        **end for**
17:        **return** $\mathbf{x}$
18: **end procedure**
19:
20: **procedure** GET_LANE_ASSIGNMENTS($\mathbf{T}, \mathcal{G}$)
21:    Initialize empty assignment list: $\mathbf{a} \leftarrow [\,]$
22:    **for** Lane segment l in $\mathcal{G}$ **do**
23:        **if** $\boldsymbol{\tau}^{T_f}$ in lane boundaries of l **then**
24:            Calculate the shortest distance d from $\boldsymbol{\tau}^{T_f}$ to the centerline of l
25:            Calculate assigned point s on lane segment l ▷ Similiar to Frenet s
26:            Calculate orientation α_{traj} of trajectory at $\boldsymbol{\tau}^{T_f}$ and orientation α_l of lane segment at s
27:            Calculate orientation difference $\Delta\alpha \leftarrow |\text{atan2}\left(\sin(\alpha_{\text{traj}} - \alpha_l), \cos(\alpha_{\text{traj}} - \alpha_l)\right)|$
28:            Calculate orientation assignment confidence $p_\alpha \leftarrow \max\left(0, 1 - \frac{\Delta\alpha}{c_{\text{orient}}}\right)$ ▷ We use $c_{\text{orient}} = \pi$
29:            Calculate distance assignment confidence $p_d \leftarrow \max\left(0, 1 - \frac{d}{c_{\text{dist}}}\right)$ ▷ We use $c_{\text{dist}} = 5\,\text{m}$ [19]
30:            Calculate combined assignment confidence $p \leftarrow w \cdot p_d + (1 - w) \cdot p_\alpha$ ▷ We use $w = 0.5$ (equal weighting)
31:            $\mathbf{a}$.insert((l, s, p))
32:        **end if**
33:    **end for**
34:    **return** $\mathbf{a}$
35: **end procedure**

A. Algorithm

Algorithm 1 provides pseudocode of our metric for the evaluation of a single sequence. Inputs are the ground-truth future $\mathbf{T}_{\text{gt}}$, the multi-modal predictions $\mathbf{T}_{\text{pred}}$ and the lane graph $\mathcal{G}$. Output is a list $\mathbf{x}$ that contains the labels 1 (miss) or 0 (hit) per predicted mode.

At a high level, the algorithm works as follows: The ground-truth endpoint gets assigned to a lane segment, more precisely to a point on the centerline of a lane segment (Line 10). Each predicted trajectory similarly gets assigned to lane segments (Line 13). For the predictions, multiple assignments are possible if multiple lane segments have a similar assignment confidence. This allows the handling of overlapping lane segments. If the distance along $\mathcal{G}$ from the assigned point of the ground-truth to any of the assigned points of the prediction is smaller than a velocity-dependent threshold s_{hit}, the prediction is a hit (label 0). Otherwise, it is a miss (label 1).

There are two special cases that are not defined in Algorithm 1: If there is no valid lane assignment for the ground-truth (e.g., ground-truth is outside of the drivable space), we fall back to a Euclidean MR and determine whether a prediction is a hit or miss by checking whether the predicted endpoint is within a radius of s_{hit} to the ground-truth endpoint or not. If there is a valid lane assignment for the ground-truth but not for a predicted trajectory, the prediction is always a miss (label 1).

In order to calculate LMR, misses are accumulated over the dataset $\mathcal{D}$. Algorithm 2 provides pseudocode for this accumulation, which follows the principle of the original Euclidean MR. LMR$_{@1}$ is defined as the ratio of sequences where the $k = 1$ mode (mode with the highest confidence) is labeled as a miss. LMR$_{@k}$ is defined as the ratio of sequences where all k modes are labeled as a miss.

B. Implementation Details

We implement our metric in Python. The implementation is parallelized on a sequence-level, meaning that Line 8 in Algorithm 2 gets executed multiple times in parallel.

In order to allow an efficient assignment of trajectories to centerlines of lane segments, an R-tree is used to query

Algorithm 2 Lane Miss Rate calculation over a full dataset

1: **Input**
2:     $\mathcal{D}$ Dataset, $|\mathcal{D}| = d$
3: **Output**
4:     LMR   Lane Miss Rate
5: **procedure** GET_LANE_MISS_RATE($\mathcal{D}$)
6:     Initialize empty miss list: $\mathbf{X} \leftarrow [\,]$
7:     **for** $(\mathbf{T}_{\text{gt}}, \mathbf{T}_{\text{pred}}, \mathcal{G})$ in $\mathcal{D}$ **do**
8:         $\mathbf{X}$.insert(GET_IS_MISS($\mathbf{T}_{\text{gt}}, \mathbf{T}_{\text{pred}}, \mathcal{G}$))
9:     **end for**
10:    Convert list of lists to 2D-array $\mathbf{X} \leftarrow$ TO_ARRAY($\mathbf{X}$),
        $\mathbf{X} \in \mathcal{R}^{d \times k}$
11:    $\text{LMR}_{@1} = \frac{\text{sum}(\mathbf{X}[:,0])}{d}$
12:    $\text{LMR}_{@k} = \frac{\text{sum}(\text{all}(\mathbf{X},\text{axis}=1))}{d}$
13:    **return** LMR
14: **end procedure**

---

lane segments around a given point (Algorithm 1, Line 22). Therefore, lane centerlines are represented with minimum bounding rectangles. This enables an efficient querying of centerlines' rectangles that intersect with the region around a defined point.

Finding valid paths along the lane graph $\mathcal{G}$ (Algorithm 1, Line 14) is done using a depth-first search. We only allow a traversal via succeeding and preceding lane segments.

The values of c_{scale} and c_{const} are oriented on the original MR, which has a fixed Euclidean threshold of $2\,\text{m}$. They are chosen so that $s_{\text{hit}} \approx 2\,\text{m}$ for $v_{\text{gt}} = 6.67\,\text{m/s}$, which corresponds to the average agent velocity in the validation split of the dataset described in Section V-A.

V. EXPERIMENTS

In this section, we use our proposed metric for the evaluation of trajectory prediction models. This includes the discussion of quantitative and qualitative results.

A. Dataset

Experiments are carried out on the large-scale Argoverse 2 Motion Forecasting Dataset [8], containing $199\,908$ sequences for training, $24\,988$ for validation and $24\,984$ for testing. Each sequence contains a High Definition (HD) map and the tracked states of agents in the surrounding of an autonomous vehicle. These states are provided over a duration of $11\,\text{s}$ and sampled with $10\,\text{Hz}$. Given the initial $5\,\text{s}$ of a sequence, the goal is to predict the trajectory of the remaining $6\,\text{s}$ of one selected agent, namely the focal agent.

B. Metrics

To allow a comparison of our newly introduced lane distance-based metric, we additionally use the most established Euclidean distance-based metrics for the evaluation of trajectory prediction models, namely minADE, minFDE and MR. For MR, the most common definition with a fixed threshold of $2\,\text{m}$ is used. Evaluation is done for single- ($k = 1$) and multi-modal ($k = 6$) prediction. We refer to Section II-A for a detailed explanation of these metrics.

The evaluation is limited to vehicle-like agents only, meaning that only agents of type vehicle, motorcyclist and bus are considered.

C. Trajectory Prediction Models

We reimplement three different state-of-the-art trajectory prediction models on Argoverse 2 and benchmark them in order to compare our proposed LMR with the most widely used Euclidean distance-based metrics. All models provide publicly available code for Argoverse 1. Argoverse 2, however, is not limited to vehicles only, which is why we add a timestep-wise one-hot encoding of each agent's class to the input of all models. The training protocols are kept the same as in the original publications.

CRAT-Pred [3] is a map-free prediction model that achieves state-of-the-art performance without making use of map information. Agent trajectories are encoded via a long short-term memory. Graph convolution and self-attention are used to aggregate temporal agent information with information of surrounding agents, namely the social context. Linear residual decoders are used to predict trajectories.

HiVT [20] consists of a local and a global encoder. The local encoder first uses timestep-wise self-attention and a subsequent temporal transformer to encode the trajectory of an agent under consideration of its surrounding agents. These local encodings are then fused with information of the HD map. Local encoding is done for each agent in a scene separately. A subsequent global encoder allows for an information exchange between the encodings resulting from the local encoder. Multilayer perceptrons are used to predict trajectories. Due to the computational complexity of the timestep-wise encoding of each agent's trajectory, including its social context given by surrounding agents, we limit the motion history to the last $2\,\text{s}$. This should have little impact on the results, as prior work in the field of learning-based pedestrian trajectory prediction shows that the deprivation of a long motion history does not lead to prediction degradation [21].

LaneGCN [2] represents information of the HD map in a lane graph and uses graph convolution to extract information from this lane graph. Agent trajectories are encoded via 1D-convolution neural networks and feature pyramid networks. Four fusion cycles are used to fuse this information with information of the lane graph. Predictions are conducted with linear residual decoders.
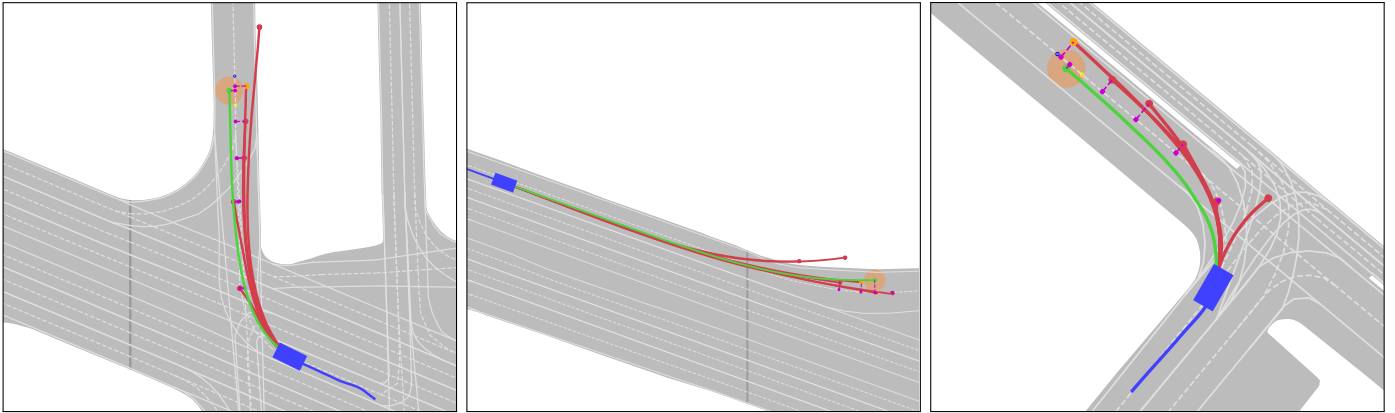
D. Quantitative Results

Table I shows quantitative results on the Argoverse 2 validation split. As described in Section IV-B, thresholds were chosen to make LMR comparable to MR. E.g., for CRAT-Pred the $\text{MR}_{@1}$ is 75.69% and the $\text{LMR}_{@1}$ is 74.27%. According to the Euclidean distance-based metrics, HiVT performs better with an $\text{MR}_{@1}$ of 71.82% and LaneGCN even more with an $\text{MR}_{@1}$ of 71.14%. The same holds for our lane distance-based metric with an $\text{LMR}_{@1}$ of 70.21% for HiVT and an $\text{LMR}_{@1}$ of 68.63% for LaneGCN. An interesting observation is that LMR

Model	$k = 1$				$k = 6$			
	minADE	minFDE	MR	LMR	minADE	minFDE	MR	LMR
CRAT-Pred	2.44	6.40	75.69	74.27	1.29	2.76	42.60	44.29
HiVT	2.31	6.23	71.82	70.21	0.97	1.99	29.97	33.30
LaneGCN	2.22	6.00	71.14	68.63	0.90	1.71	25.87	29.72
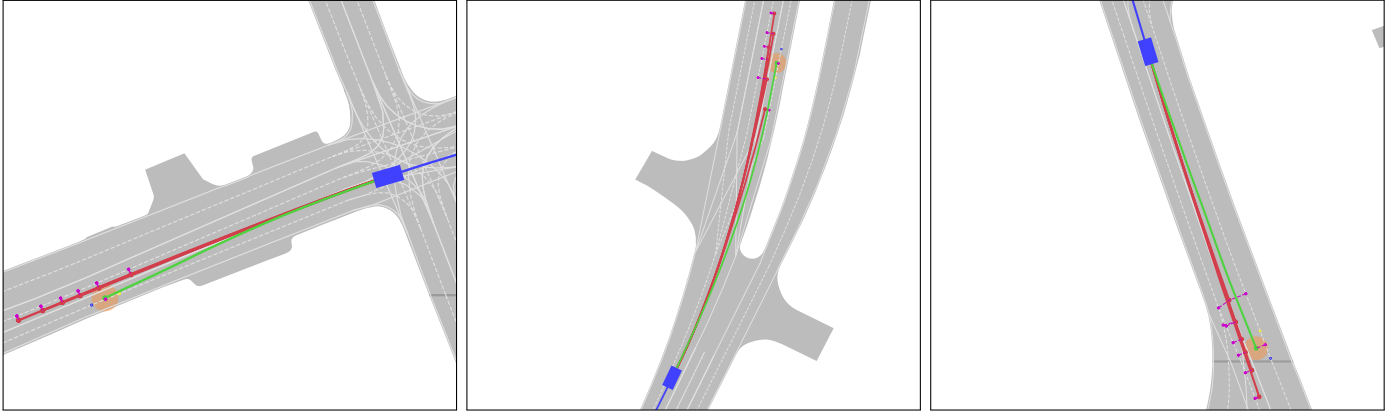
(a) Sequences that are a miss in terms of our Lane Miss Rate but not in terms of the Euclidean Miss Rate

(b) Sequences that are a miss in terms of the Euclidean Miss Rate but not in terms of our Lane Miss Rate

Fig. 2. Qualitative results of our Lane Miss Rate with LaneGCN: The past observed trajectory of the focal agent is colored in blue, the ground-truth future trajectory in green. Predictions are colored in red. Endpoints of ground-truth and predictions are marked with a dot. The assignments of the ground-truth and the predicted trajectories to the centerlines of lane segments are colored in purple. Predictions with an assignment that falls in between the blue and yellow dot on the ground-truth centerline yield a hit and vice versa. Predicted endpoints that yield a hit according to this definition are colored in orange instead of red. For comparison, the definition of the Euclidean Miss Rate is colored in light orange and centered around the ground-truth endpoint.

preserves the order of the Euclidean distance-based metrics in all quantitative results.

Another aspect is that the relative deviations between models differ for LMR compared to the other metrics. For instance, the $MR_{@6}$ is 29.97% for HiVT and 25.87% for LaneGCN, which is a relative increase of 15.85%. However, the $LMR_{@6}$ is 33.30% for HiVT and 29.72% for LaneGCN, which is a relative increase of only 12.05%. The values indicate a lower effective difference in performance between HiVT and LaneGCN, which could only be identified with our new LMR metric. Also, this confirms the benefit gained from an additional metric that uses lane distance instead of

Euclidean distance. We suggest investigating the performance of trajectory prediction models that use a lane-based loss, e.g., [22]. Additionally, we suggest investigating encoders that use information beyond lane segments, e.g., [23], and see how this implicitly influences our lane distance-based metric. Due to the lack of publicly available code, this is beyond the scope of this paper.

E. Qualitative Results

Fig. 2 shows qualitative examples where the definition of our $LMR_{@6}$ leads to different results than the standard Euclidean $MR_{@6}$.

Fig. 2 (a) shows sequences that yield a miss for all predicted trajectories in terms of LMR but not in terms of MR. In all three sequences, the predictions do not cover the lane of the ground-truth, hence LMR results in a miss. This illustrates that LMR implicitly weights Euclidean error relative to the lanes, by assigning ground-truth and predictions to centerlines of lane segments. MR, however, is dependent on Euclidean distance and therefore weights error equally in all directions. This results in the predictions not resulting in a miss, despite being located on the wrong lane.

Fig. 2 (b) shows sequences that yield a miss for all predicted trajectories in terms of MR but not in terms of LMR. All three sequences show a clear trend: The predictions are located on the correct lane but are outside the $2\,\mathrm{m}$ MR radius. Again, this illustrates that LMR implicitly weights Euclidean error relative to the lanes. In this case, predictions are not labeled as a miss, because they are located on the correct lane and therefore cover the intent of the predicted vehicle.

VI. CONCLUSION

We propose LMR, a novel lane distance-based metric for the evaluation of trajectory prediction models. Quantitative and qualitative results on three state-of-the-art trajectory prediction models confirm the validity of this additional metric. The benefit of LMR is that components of the Euclidean error are weighted relative to the underlying lanes. This way, LMR extends the set of existing purely geometric metrics and goes into the direction of capturing intents of traffic agents.

Our publicly available source code of LMR for Argoverse 2 enables other researchers to evaluate their approaches with this lane distance-based metric.

REFERENCES

[1] J. Gao, C. Sun, H. Zhao, Y. Shen, D. Anguelov, C. Li, and C. Schmid, "Vectornet: Encoding hd maps and agent dynamics from vectorized representation," in *2020 IEEE/CVF Conference on Computer Vision and Pattern Recognition (CVPR)*, 2020, pp. 11 522–11 530.

[2] M. Liang, B. Yang, R. Hu, Y. Chen, R. Liao, S. Feng, and R. Urtasun, "Learning lane graph representations for motion forecasting," in *Computer Vision – ECCV 2020*, A. Vedaldi, H. Bischof, T. Brox, and J.-M. Frahm, Eds. Cham: Springer International Publishing, 2020, pp. 541–556.

[3] J. Schmidt, J. Jordan, F. Gritschneder, and K. Dietmayer, "Crat-pred: Vehicle trajectory prediction with crystal graph convolutional neural networks and multi-head self-attention," in *2022 IEEE International Conference on Robotics and Automation (ICRA)*, 2022, pp. 7799–7805.

[4] T. Phan-Minh, E. C. Grigore, F. A. Boulton, O. Beijbom, and E. M. Wolff, "Covernet: Multimodal behavior prediction using trajectory sets," in *2020 IEEE/CVF Conference on Computer Vision and Pattern Recognition (CVPR)*, 2020, pp. 14 062–14 071.

[5] N. Djuric, V. Radosavljevic, H. Cui, T. Nguyen, F.-C. Chou, T.-H. Lin, N. Singh, and J. Schneider, "Uncertainty-aware short-term motion prediction of traffic actors for autonomous driving," in *2020 IEEE Winter Conference on Applications of Computer Vision (WACV)*, 2020, pp. 2084–2093.

[6] M.-F. Chang, J. Lambert, P. Sangkloy, J. Singh, S. Bak, A. Hartnett, D. Wang, P. Carr, S. Lucey, D. Ramanan, and J. Hays, "Argoverse: 3d tracking and forecasting with rich maps," in *2019 IEEE/CVF Conference on Computer Vision and Pattern Recognition (CVPR)*, 2019, pp. 8740–8749.

[7] S. Ettinger, S. Cheng, B. Caine, C. Liu, H. Zhao, S. Pradhan, Y. Chai, B. Sapp, C. R. Qi, Y. Zhou, Z. Yang, A. Chouard, P. Sun, J. Ngiam, V. Vasudevan, A. McCauley, J. Shlens, and D. Anguelov, "Large scale interactive motion forecasting for autonomous driving: The waymo open motion dataset," in *2021 IEEE/CVF International Conference on Computer Vision (ICCV)*, 2021, pp. 9710–9719.

[8] B. Wilson, W. Qi, T. Agarwal, J. Lambert, J. Singh, S. Khandelwal, B. Pan, R. Kumar, A. Hartnett, J. Kaesemodel Pontes, D. Ramanan, P. Carr, and J. Hays, "Argoverse 2: Next generation datasets for self-driving perception and forecasting," in *Proceedings of the Neural Information Processing (NeurIPS) Systems Track on Datasets and Benchmarks*, vol. 1, 2021.

[9] N. Lee, W. Choi, P. Vernaza, C. B. Choy, P. H. S. Torr, and M. Chandraker, "DESIRE: distant future prediction in dynamic scenes with interacting agents," in *2017 IEEE Conference on Computer Vision and Pattern Recognition (CVPR)*, 2017, pp. 2165–2174.

[10] A. Gupta, J. Johnson, L. Fei-Fei, S. Savarese, and A. Alahi, "Social GAN: socially acceptable trajectories with generative adversarial networks," in *2018 IEEE/CVF Conference on Computer Vision and Pattern Recognition (CVPR)*, 2018, pp. 2255–2264.

[11] N. Rhinehart, K. M. Kitani, and P. Vernaza, "R2p2: A reparameterized pushforward policy for diverse, precise generative path forecasting," in *Computer Vision – ECCV 2018*, V. Ferrari, M. Hebert, C. Sminchisescu, and Y. Weiss, Eds. Cham: Springer International Publishing, 2018, pp. 794–811.

[12] N. Rhinehart, R. Mcallister, K. Kitani, and S. Levine, "Precog: Prediction conditioned on goals in visual multi-agent settings," in *2019 IEEE/CVF International Conference on Computer Vision (ICCV)*, 2019, pp. 2821–2830.

[13] G. W. Brier, "Verification of forecasts expressed in terms of probability," *Monthly Weather Review*, vol. 78, no. 1, pp. 1–3, 1950.

[14] R. A. Yeh, A. G. Schwing, J. Huang, and K. Murphy, "Diverse generation for multi-agent sports games," in *2019 IEEE/CVF Conference on Computer Vision and Pattern Recognition (CVPR)*, 2019, pp. 4605–4614.

[15] B. Ivanovic and M. Pavone, "The trajectron: Probabilistic multi-agent trajectory modeling with dynamic spatiotemporal graphs," in *2019 IEEE/CVF International Conference on Computer Vision (ICCV)*, 2019, pp. 2375–2384.

[16] H. Cui, T. Nguyen, F.-C. Chou, T.-H. Lin, J. Schneider, D. Bradley, and N. Djuric, "Deep kinematic models for kinematically feasible vehicle trajectory predictions," in *2020 IEEE International Conference on Robotics and Automation (ICRA)*, 2020, pp. 10 563–10 569.

[17] J. Philion, A. Kar, and S. Fidler, "Learning to evaluate perception models using planner-centric metrics," in *2020 IEEE/CVF Conference on Computer Vision and Pattern Recognition (CVPR)*, 2020, pp. 14 052–14 061.

[18] B. Ivanovic and M. Pavone, "Rethinking trajectory forecasting evaluation," 2021.

[19] J. Schmidt, J. Jordan, D. Raba, T. Welz, and K. Dietmayer, "Meat: Maneuver extraction from agent trajectories," in *2022 IEEE Intelligent Vehicles Symposium (IV)*, 2022, pp. 1810–1816.

[20] Z. Zhou, L. Ye, J. Wang, K. Wu, and K. Lu, "Hivt: Hierarchical vector transformer for multi-agent motion prediction," in *2022 IEEE/CVF Conference on Computer Vision and Pattern Recognition (CVPR)*, 2022, pp. 8823–8833.

[21] C. Schöller, V. Aravantinos, F. Lay, and A. Knoll, "What the constant velocity model can teach us about pedestrian motion prediction," *IEEE Robotics and Automation Letters*, vol. 5, no. 2, pp. 1696–1703, 2020.

[22] J. Wang, T. Ye, Z. Gu, and J. Chen, "Ltp: Lane-based trajectory prediction for autonomous driving," in *2022 IEEE/CVF Conference on Computer Vision and Pattern Recognition (CVPR)*, 2022, pp. 17 134–17 142.

[23] T. Monninger, J. Schmidt, J. Rupprecht, D. Raba, J. Jordan, D. Frank, S. Staab, and K. Dietmayer, "Scene: Reasoning about traffic scenes using heterogeneous graph neural networks," *IEEE Robotics and Automation Letters*, vol. 8, no. 3, pp. 1531–1538, 2023.